



## Research Article

<https://doi.org/10.1631/jzus.A2500648>

# High-sensitivity flexible iontronic pressure sensor for pulse signal detection and underwater intelligent communication

Menghui XIANG<sup>1,2\*</sup>, Cong ZHAI<sup>2\*✉</sup>, Congcong HAO<sup>3\*✉</sup>, Guirong WU<sup>1</sup>, Jin CHAI<sup>2,4</sup>, Yunlong ZHAO<sup>1</sup>, Zekai HUANG<sup>1</sup>, Bin YAO<sup>1,2</sup>, Heying ZHANG<sup>3</sup>, Mengran LIU<sup>5</sup>, Lei NIE<sup>5</sup>, Xiewen WEN<sup>6</sup>, Chenyang XUE<sup>1,2</sup>, Libo GAO<sup>1✉</sup>

<sup>1</sup>Pen-Tung Sah Institute of Micro-Nano Science and Technology, and Discipline of Intelligent Instrument and Equipment, Xiamen University, Xiamen 361102, China

<sup>2</sup>Laoshan Laboratory, Qingdao 266237, China

<sup>3</sup>Key Laboratory of Instrumentation Science & Dynamic Measurement Ministry of Education, North University of China, Taiyuan 030051, China

<sup>4</sup>College of Chemistry and Chemical Engineering, Xiamen University, Xiamen 361102, China

<sup>5</sup>Hubei Key Laboratory of Modern Manufacturing Quantity Engineering, School of Mechanical Engineering, Hubei University of Technology, Wuhan 430068, China

<sup>6</sup>Department of ISE, University Research Facility in 3D Printing, and State Key Laboratory of Ultra-precision Machining Technology, The Hong Kong Polytechnic University, Hong Kong, China

**Abstract:** Flexible pressure sensors have become pivotal in the advancement of wearable electronics, underwater monitoring, and human-machine interfaces (HMI), particularly when augmented by artificial intelligence. Nevertheless, the development of a unified sensing platform capable of seamless operation in both terrestrial health monitoring and aquatic communication environments remains a significant challenge. To address this issue, a highly sensitive, flexible ionic pressure sensor featuring a micro-pyramidal architecture was developed. The device is fabricated using molding involving a bespoke ionic ink composite comprising carbon nanotubes (CNTs) and ionic liquids as the sensing layer. This layer is then sandwiched between screen-printed silver electrodes. The sensor demonstrates exceptional performance metrics, including high sensitivity (370 kPa<sup>-1</sup>), rapid response/recovery times (20 ms), and outstanding reliability (about 20000 cycles). In the domain of wearable health monitoring, the sensor demonstrated its capacity to discern faint human pulse signals. The integration of established principles from traditional Chinese pulse-taking methodologies was successful in identifying optimal pressure points, thereby facilitating the acquisition of high-fidelity pulse waveforms. Concurrently, within the domain of underwater intelligent communication, the sensor was used to sense Morse code signals, which were then accurately classified through a deep learning algorithm. This research has established a reliable method for covert messaging and has significantly augmented the potential for biological monitoring in aquatic environments. This work not only validates the sensor's high performance but also demonstrates its dual-functionality, seamlessly connecting human healthcare with intelligent underwater interaction and significantly broadening the scope of application of flexible sensing technology.

**Key words:** Flexible pressure sensor; Underwater sensing; Iontronic sensor; Machine learning

## 1 Introduction

Recent years have seen a significant advancement in the field of flexible sensors, largely

driven by their extensive applications in human physiological monitoring (Yang et al., 2023; Teng et al., 2024; Zhao et al., 2024) and motion tracking (Ren et al., 2021; Zhu et al., 2024; Zhang et al., 2024; Liang et al., 2025; Liu et al., 2024). Concurrently, continuous technological innovations have significantly enhanced their sensitivity and operational stability. In essence, flexible sensors substitute conventional rigid materials with compliant counterparts (Lin et al., 2025; Min et al., 2023), encompassing piezoresistive (Xiang et al., 2024; Li et al., 2025), capacitive (Ma et al., 2023; Liu et al.,

✉ Cong ZHAI, [OliverChild@hotmail.com](mailto:OliverChild@hotmail.com)

Congcong HAO, [20210093@nuc.edu.cn](mailto:20210093@nuc.edu.cn)

Libo GAO, [lbgao@xmu.edu.cn](mailto:lbgao@xmu.edu.cn)

\* These authors contributed equally to this work

Received Dec. 11, 2025; Revision accepted Feb. 4, 2026;

Crosschecked

2025), and triboelectric principles (Chang et al., 2025; Sun et al., 2025). Capacitive sensors have attracted particular attention due to their structural simplicity, low power consumption, and excellent stability. Li et al. (2025) proposed a flexible capacitive sensor with a micro-pyramidal structure that can detect subtle physiological signals, such as heart rate, facial expressions and joint movements. Liu et al. (2025) attained a substantial advancement in sensitivity by devising a hybrid system incorporating CNTs and thermally expandable microspheres. They reported a twofold enhancement in sensitivity compared with systems that used CNTs alone. In addition, Kurup et al. (2022) advanced material design through the use of graphene-coated PDMS porous foam, thereby fabricating a sensor capable of detecting minute pressure variations. This finding underscores the sensor's potential for wearable biomedical applications.

However, conventional parallel-plate capacitive sensors are subject to inherent limitations, including relatively low sensitivity (typically  $< 1 \text{ kPa}^{-1}$ ) and instability due to environmental factors such as humidity, temperature, and parasitic capacitance. To address these challenges, iontronic sensing has emerged as a transformative paradigm (Nie et al., 2015; Nie et al., 2012; Guo et al., 2025; Cheng et al., 2022). This approach facilitates the formation of electrical double layers (EDLs) at the interface, generating nanoscale double-layer capacitances. This mechanism yields remarkably elevated capacitance per unit area (frequently  $> 1 \mu\text{F cm}^{-2}$ ) and sensitivity (typically  $10\text{-}100 \text{ kPa}^{-1}$ ), demonstrating substantial superiority over conventional parallel-plate structures. Consequently, this mechanism has prompted many researchers to focus on the stronger high sensitivity of ion-based sensors and conduct related application research. For instance, Yang et al. (2024) focused on enhancing the sensitivity of ion-based pressure sensors. They engineered an ultra-sensitive pressure sensor using thermally expandable microspheres and constructed a flexible array capable of high-resolution radial artery pulse detection. Subsequent studies prompt a gradual shift in research focus from the initial emphasis on basic performance enhancements, such as sensitivity, to multifunctional integration and intelligent system applications. For instance, Yang et al. (2023) initiated research on multifunctional

integration and developed an ion-based sensor with temperature and pressure decoupling, which demonstrated significant application value in the field of human-computer interaction. In their subsequent research, they integrated intelligent system applications, developed a machine learning-enhanced modular ionic skin, and established a versatile framework for operator identification and robotic tactile recognition in next-generation HMI applications (Yang et al., 2025). Zhao et al. (2024) also conducted research on multifunctional integration and intelligent system applications based on high sensitivity. These applications integrate multi-channel active pressure for signal acquisition and perform personalized blood pressure prediction based on artificial intelligence.

Concurrently, flexible pressure sensors have been increasingly adapted for underwater applications, presenting both unique opportunities and challenges within aquatic environments. The implementation of sensors in underwater environments requires high standards of waterproofing, pressure resistance, signal fidelity, and associated properties. Notably, the ability to withstand submersion represents a pivotal challenge. At present, technical solutions that demonstrate effective waterproof capabilities encompass mainly gels, mechanical structures, and other waterproof materials. For instance, Yang et al. (2024) fabricated hydrogel electrodes composed of MXene and ionic liquids, integrating them into a sensor capable of continuous operation for a period of 60 days. Their device offers novel pathways for flow field monitoring and aquatic tagging. Zhao et al. (2024) proposed a capacitive hydrophone (CH) based on mechanical structure encapsulation, specifically designed for high-sensitivity detection of low-frequency underwater acoustic signals, demonstrating the ability of a CH to detect ships and underwater sounds. In our previous research, we fabricated two types of underwater capacitive pressure sensors based on waterproof material encapsulation. One of these sensors was designed for monitoring in shallow seas, while the other was designed for monitoring in deep seas (Xiang et al., 2025; Wang et al., 2024). A comparative analysis of the three underwater encapsulation methods revealed that the gel-based process is relatively cumbersome, while the mechanical structure-based approach

necessitates the design of a tight waterproof structure and the processing of metal parts. The encapsulation of flexible,



Fig. 1 Overall application and preparation process of the sensor: (a) sensor layered structure diagram and detailed manufacturing process; (b-c) schematic diagram of sensor attached places; (d) schematic diagram of underwater communication

waterproof materials has seen a surge in popularity, owing to its numerous advantages, including ease of

access and preparation. This method has been shown to achieve a balance between critical characteristics

such as cost, pressure resistance, and signal fidelity. Nevertheless, research in this domain exhibits certain deficiencies with respect to cross-media generalization and integrated land-sea intelligent sensing platforms. Most reported sensors can perform distinct functions in two distinct domains: underwater communication and physiological health monitoring. While these limitations do not significantly impact the sensors' fundamental capabilities, they do impose constraints on their versatility and range of application. The sensor described in this paper represents a development of our previous research on underwater pressure sensors. On the one hand, it can be used in both air and underwater media after undergoing waterproof encapsulation. On the other hand, the concurrent implementation of underwater communication and human physiological signal monitoring enables the sensor to assume a more pivotal role in swimming, diving, and underwater tasks, such as the timely provision of alerts to divers in cases of imminent peril.

In this study, sensor electrodes were fabricated using screen-printed conductive silver paste, while the ion-sensitive layer was mainly formulated from a composite ink of CNTs and ionic liquids. The sensor's layered structure and simplified manufacturing method are shown in Fig. 1a. To enhance sensitivity, a micro-pyramidal architecture was engineered onto the sensing layer via a molding process, followed by laser cutting for device shaping. This fabrication strategy not only supports high customization but also facilitates scalable batch production, significantly widening the sensor's potential adoption. The device demonstrates robust functionality across diverse environments, leveraging its exceptional sensitivity. The sensor can effectively detect different signals when attached in different places (Figs. 1b and 1c). The application of principles derived from traditional Chinese medicine (TCM) – specifically the technique of using graduated pressure to ascertain the optimal detection pressure – has facilitated the acquisition of high-fidelity pulse waveforms. To extend the operational scope of the sensor to aquatic environments, the sensor was encapsulated in an ultra-thin medical-grade adhesive film. In subsequent experiments conducted underwater (Fig. 1d), the sensor showed the capacity to sense Morse code signals, which were accurately decoded by means of a

deep learning algorithm. The integration of flexible sensing with intelligent signal processing has the potential to significantly expand the application scope of the sensor.

## 2 Methods

### 2.1 Materials and Equipment

The electrode material selected for the sensor was stretchable conductive silver paste (Shanghai Ouyi Organic Photoelectric Materials Co., Ltd.). The composition of the sensor's sensitive layer material included a blend of thermoplastic polyurethane (TPU, supplied by Dongguan Zhangmutou Ruixiang Polymer Materials Operation Department), carbon nanotubes (CNTs, procured from Suzhou Carbon Peak Graphene Technology Co., Ltd.), and an ionic liquid (1-ethyl-3-methylimidazolium bis(trifluoromethylsulfonyl) imide, EMIM, obtained from Aladdin, Shanghai, China). The organic solvent used was DMF (N, N-dimethylformamide, Aladdin Company).

A series of experiments were conducted to assess the mechanical and electrical properties of the sensor. The experimental apparatus included a digital inductance, capacitance and resistance (LCR) meter (TH2840B, Tonghui) and a mechanical testing machine (ZQ-990B, Zhiqiu). The electrodes, sensitive layer structure, and element distribution were observed using a scanning electron microscope (Carl Zeiss, G300).

### 2.2 Sensor Fabrication

The simplified sensor fabrication process is illustrated in Fig. 1a (for more details, refer to the supplementary material Fig. S1). First, polyethylene terephthalate substrates were laser-cut into the desired geometry and plasma-treated to enhance surface adhesion. Conductive silver paste was then deposited onto the substrates via screen printing, followed by curing in a vacuum oven at 80 °C for 10 min to finalize the electrodes. The preparation of the ionic sensing membrane involved the dissolution of TPU pellets in DMF at a ratio of 1:5 under magnetic stirring (80 °C, 220 rpm) for a duration of 30 min, with the objective of achieving a homogeneous

solution. Subsequently, 1 mL of the ionic liquid EMIM was added dropwise to prevent agglomeration. Finally, CNTs were introduced to the

mixture. The slurry was stirred at a rate of 200 rpm for a period of 10 min, then subjected to high-frequency

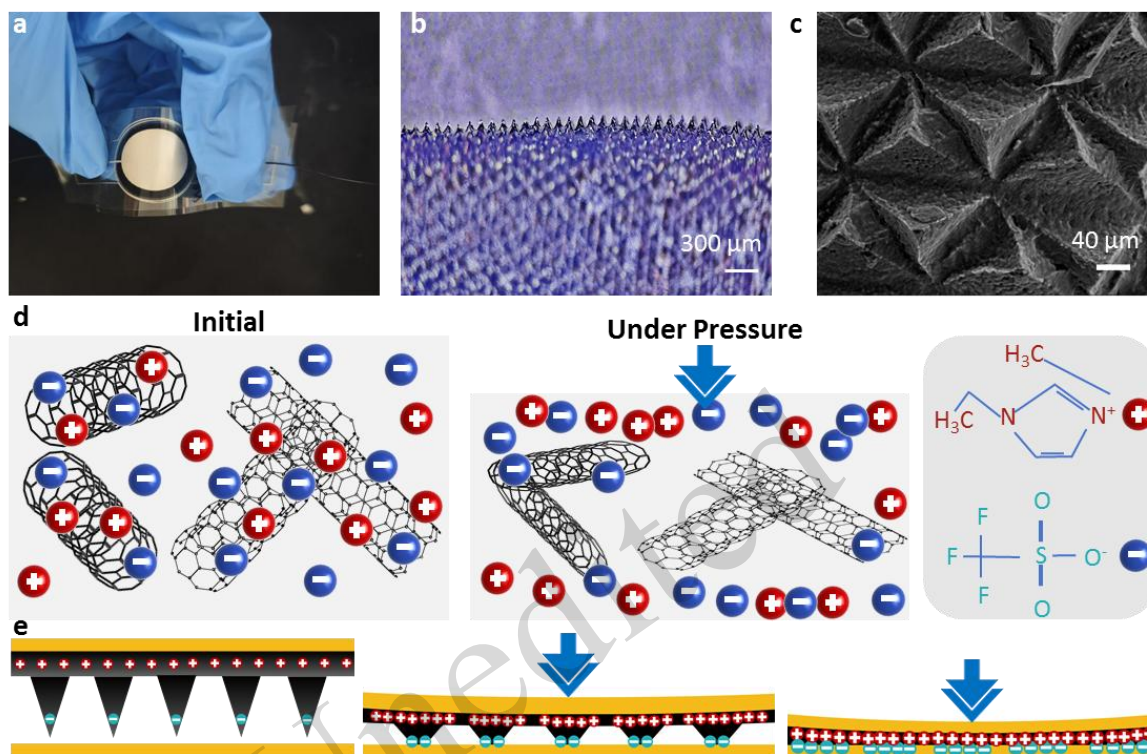


**Fig. 2** Sensor mechanism: (a) physical diagram of the sensor; (b-c) microstructural diagram of sensitive layer; (d) schematic diagram of sensor micro-mechanism; (e) sensor macro-mechanism diagram

ultrasonication to ensure a uniform dispersion of the conductive fillers. The resulting ionic composite was cast into a prefabricated mold and subjected to a spin-coating process, which ensured uniform film thickness. Following a drying process in a vacuum oven at 80 °C for 30 min, the freestanding ionic film was peeled from the mold. The sensor assembly was completed by the methodical placement of the ionic film between two silver electrodes, with the use of 3M double-sided adhesive tape functioning as a spacer to delineate the active sensing area and facilitate adhesion of the layers. Fig. 1a provides an exploded view of the sensor's layered architecture. To optimize pressure sensitivity, a micro-pyramidal structure was engineered within the sensing layer using a molding technique. An optical photograph of the fully fabricated sensor is presented in Fig. 2a. The microstructural details are highlighted in Fig. 2b, where a cross-sectional optical micrograph captures the well-defined pyramidal profile of the ionic membrane. Scanning electron microscopy (SEM)

further elucidates this morphology in Fig. 2c, confirming the structural uniformity of the pyramids. After the morphological characterization, energy dispersive spectroscopy (EDS) was used to evaluate the elemental composition. To eliminate potential topographic artefacts in the EDS mapping caused by the height variation of the micro-pyramids, a flat, microstructure-free film was synthesized for this analysis. The unique N and F elements present in the ionic liquid exhibit a uniform and dense distribution throughout the sensitive layer matrix (Fig. S2), further verifying the uniform distribution of ionic liquid and CNTs in the matrix.

### 2.3 Analysis of Sensing Mechanism

The sensing mechanism was elucidated using a dual-perspective analysis, integrating microscopic interfacial principles with macroscopic contact mechanics. Microscopically, the incorporation of ionic liquids fundamentally transforms the device from a conventional parallel-plate capacitor into an

iontronic sensor. Unlike in conventional architectures, the mobile ions present within the electrolyte facilitate the formation of EDLs at the electrode interfaces, with charge separation occurring on the nanometer scale. This mechanism yields an ultra-high specific capacitance (capacitance per unit area). Consequently, the total detected capacitance is contingent on the effective interfacial contact area. The sensor achieves baseline capacitance values in the nano-farad range (nF) because of the super-capacitive effect. This is significantly higher than the picofarad (pF) range typical of parallel-plate counterparts. This high intrinsic capacitance has been shown to significantly reduce the device's impedance, thereby minimizing its susceptibility to parasitic electromagnetic noise from the environment. Consequently, this results in a marked enhancement of both the signal-to-noise ratio and the resolution of the signal. Moreover, the tubular topology of the CNTs facilitates efficient loading and retention of the ionic liquid, ensuring robust ionic transport. For clarity, the schematic diagram has been simplified by depicting only CNTs and positive and negative ions in the sensor sensitive material (Fig. 2d). On a macroscopic level, the engineered pyramidal microstructure exerts a regulatory influence on the dynamic response of the contact area. The sensing principle is predicated on the modulation of the ion-electron interface under mechanical load. As the pressure increases, the contact area between the pyramidal features and the bottom electrode evolves through distinct regimes: initial apex contact, progressive sidewall deformation, and eventual structural saturation. This characteristic deformation behavior gives rise to a non-linear variation in contact area, which initially grows gradually, followed by a rapid expansion, and finally plateaus. This variation aligns precisely with the measured sensitivity curve of the sensor. In the initial phase, the contact area between the pyramid microstructure and the electrode is comparatively small, thus resulting in minimal alterations (Fig. 2e). The mid-term stage is characterized by the most significant changes in the contact area between the pyramid structure and the electrode, thereby optimizing sensitivity. The subsequent phase is known as the deformation saturation stage, during which the sensitivity is the least optimal.

## 3 Results and Discussion

### 3.1 Sensor Performance

The final sensor architecture was established through a series of comparative experiments aimed at optimizing the design. Initially, conductive silver paste was selected for the electrodes due to its excellent rheological properties for screen printing and scalability for mass production. To enhance performance, a hybrid composite of an ionic liquid and CNTs was used. This formulation transformed the device from a conventional parallel-plate capacitor into an EDLs-based sensor, thereby significantly enhancing sensitivity and immunity to environmental interference. To identify the optimum compromise between cost and performance, composites with various concentrations of CNTs were evaluated. The sensor attained optimal functionality with a CNTs loading of 0.1 g (3.8 wt%) (Fig. 3a). This effect can be attributed to two main factors. Firstly, an increase in the content of CNTs will lead to a continuous increase in the conductivity of the ion-sensitive layer, which may result in a larger initial capacitance of the sensor. Consequently, a higher requirement is placed on the large capacitance change required for the sensor's high sensitivity. Conversely, an increased quantity of CNTs may result in their disparate dispersion within the ion slurry, which may, in turn, diminish the deformability and mechanical stability of the ion-sensitive layer. Following confirmation of the optimal content of CNTs, an investigation was conducted into the content of the ionic liquid in the sensitive layer. With a constant CNTs content, sensitive layer slurries were prepared using 0.5 ml, 1 ml, or 2 ml of ionic liquid. A comprehensive array of experimental findings is given in Fig. S3. The results showed that 1 ml of ionic liquid was the optimal volume within the experimental parameters delineated in this study. Two potential explanations for this phenomenon are posited. First, an increase in the amount of ionic liquid may increase the initial capacitance of the sensor. This, in turn, necessitates a greater change in capacitance to achieve high sensitivity. Second, an increase in the amount of ionic liquid may result in a decrease of the elastic modulus of the composite

material. This decrease has the potential to narrow the high sensitivity range of the material and facilitate the attainment of saturation. The sensitivity profile of the

sensor exhibits three distinct regimes, governed by the deformation mechanics of the micro-pyramidal structure (Fig. 3b)

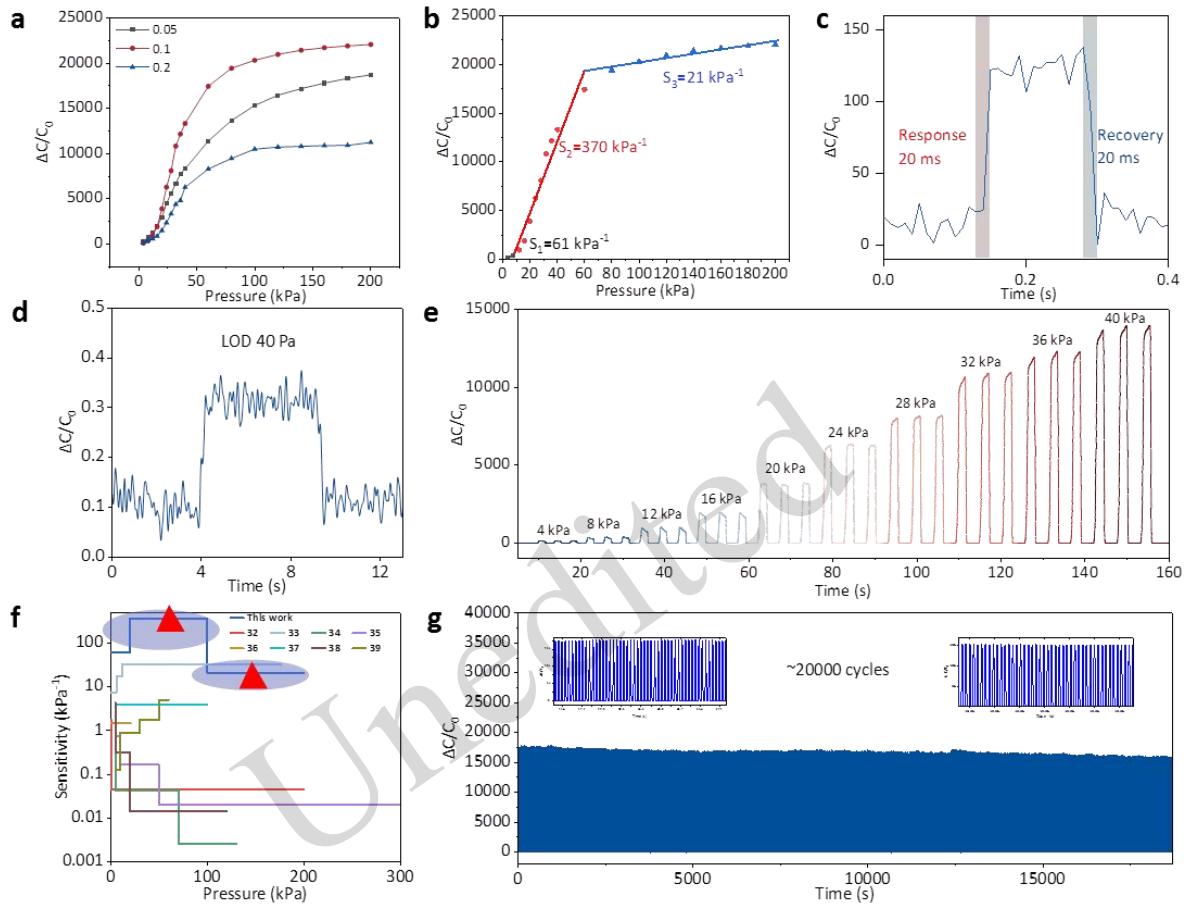


**Fig. 3** Sensor performance: (a) comparison of different ionic layers; (b) sensor sensitivity; (c) the response and recovery time of the sensor; (d) LOD of the sensor; (e) the output of the sensor under different pressures; (f) sensor performance comparison; (g) sensor output under about 20000 cycles of loading-unloading tests

(for more details of the sensitivity mechanism, please refer to the Analysis of Sensing Mechanism section). In addition, the transient characteristics of the sensor were evaluated, a critical component for effective real-time monitoring. The device exhibits rapid response and recovery times, with both measuring about 20 ms (Fig. 3c). The limit of detection (LOD) was determined through the application of subtle pressure using lightweight aluminum weights. The sensor demonstrated its capability to capture weak physiological signals, resolving pressures as low as 40 Pa (Fig. 3d). Furthermore, an assessment was conducted of the sensor's dynamic range and stability. Step-loading tests (Figs. 3e and S4) confirmed the robustness of the signal stability across various pressure gradients. Comparisons (Fig. 3f) with other

published sensors showed that our sensor achieves a superior balance between high sensitivity and a broad detection range (Guo et al., 2024; Lu et al., 2021; Jin et al., 2024; Hong et al., 2023; Lv et al., 2023; Wang et al., 2024; Yang et al., 2019; Cetin et al., 2024). Finally, the long-term durability of the sensor was validated through the implementation of cyclic loading; the sensor showed stable performance with negligible signal drift after about 20,000 cycles at 60 kPa, thereby indicating excellent operational reliability. The capacitive response of the sensor degraded after a certain number of cycles (Fig. 3g). The main cause of this degradation presumably is fatigue in the sensitive layer. Due to the relatively high velocity and substantial pressure applied during testing, the sensor was subjected to extreme and harsh

conditions that it would rarely encounter in normal use. This resulted in irreversible deformation or cracks in the microstructure of the sensitive layer

under cyclic pressure, leading to reduced compressibility and resilience, and

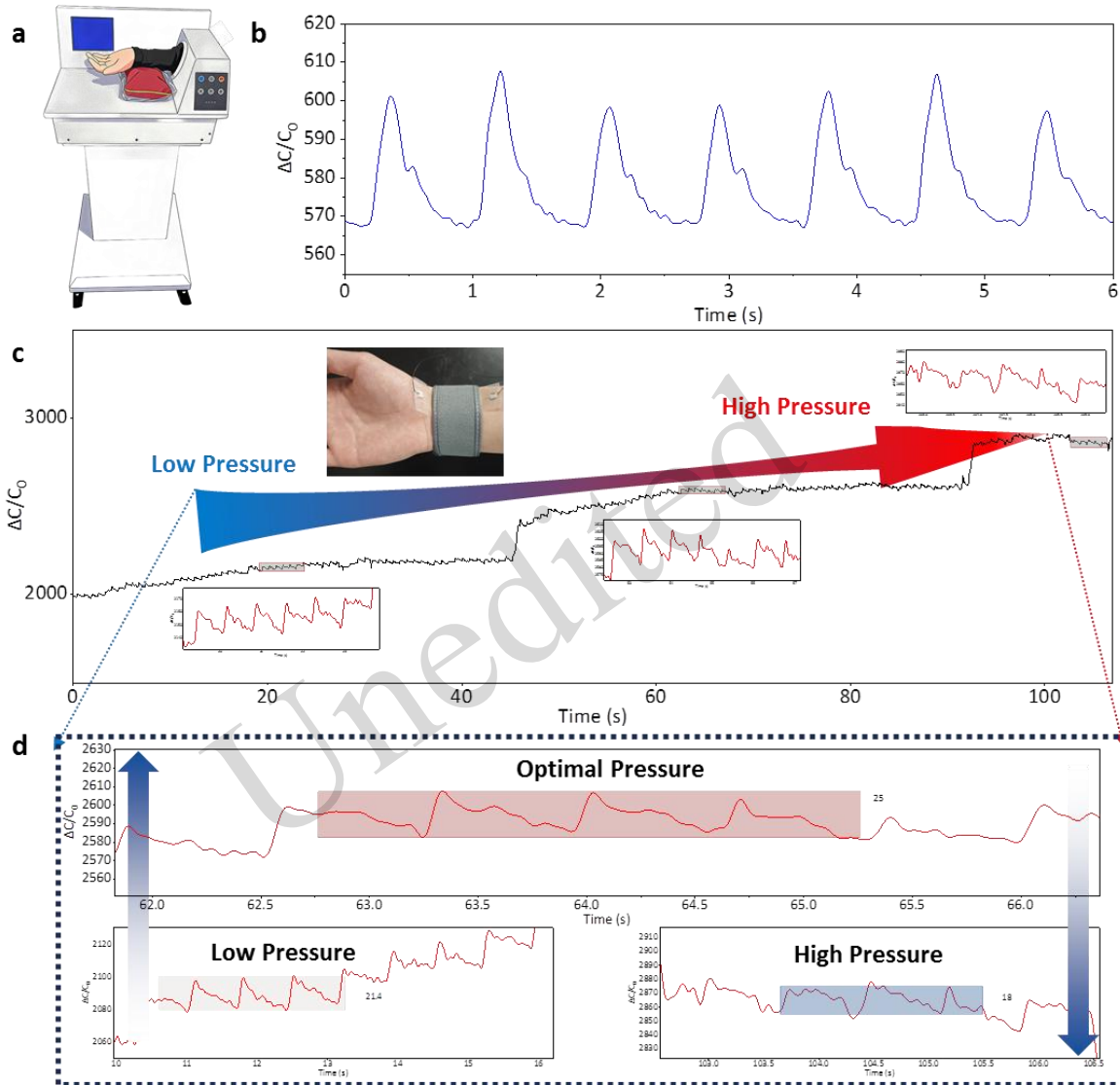


**Fig. 4** Pulse detection application of sensor: (a) standard pulse signal instrument; (b) simulated pulse signal; (c-d) actual pulse signal and locally magnified view

further performance degradation. Note that even in the presence of degradation, the performance showed a notable degree of sensitivity, and so such degradation should not have a substantial impact in practical application scenarios.

### 3.2 Pulse Signal Detection

The pulse signal originating from the heart is a significant physiological signal used for measuring human health. The signal is not only directly related to heart rate but also has the capacity to provide a

more comprehensive reflection on the health status of the human heart. In TCM, pulse diagnosis has a particularly significant emphasis. To rigorously validate the sensor's pulse detection capabilities, both simulated equipment tests and in vivo human trials were conducted. Initially, a commercial pulse signal generator (Fig. 4a) was used to assess response to standardized waveforms. Despite the simulator producing signal amplitudes that are considerably higher than those of typical human pulses, the sensor accurately resolved the waveform features. The

PQRST and other characteristics of the pulse signal were clearly visible (Fig. 4b). Subsequently, an evaluation was conducted of the sensor's capacity to capture subtle arterial pulses from a human subject. This application was inspired by the variable-pressure techniques used in TCM pulse diagnosis. Accordingly, graduated static pressure was applied to the radial artery. The sensor produced waveforms of high fidelity across a range of pressure levels (Figs. 4c and 4d). Quantitative analysis revealed that the pulse signal amplitude showed a non-monotonic trend, initially increasing and then decreasing as pressure rose. This observation is consistent with the TCM principle of an optimal pulse pressure for maximizing diagnostic accuracy. Performance tests were also conducted on the sensor under bending conditions (Fig. S5). The sensor showed a higher output under bending conditions when subjected to the same pressure. This phenomenon can be attributed, at least in part, to the sensor's increased deformation when subjected to bending conditions, which in turn leads to a more substantial capacitance change. Nevertheless, this does not have a substantial impact on the practical application scenarios of the sensor. The analysis of the experimental results indicates that sensor has the capacity to obtain human pulse signals in a variety of states, which can make a significant contribution to long-term physiological signal monitoring in future health scenarios.

### 3.3 Underwater Intelligent Communication

Following the detection of human physiological signals, the sensors were encapsulated for the purpose of testing their application in underwater intelligent communication. The underlying objective of this study was to explore the potential of underwater encapsulation to broaden the operational scope of the sensors, thereby facilitating their effective use in both air and underwater environments. The construction of the underwater intelligent communication system was intended to provide further verification of the robustness of the sensors in complex underwater environments and their ability to integrate with machine learning systems. The medical waterproof tape used in this study boasts several noteworthy characteristics, including its ultra-thin profile, remarkably strong

adhesiveness, and notable stretchability. The sensors' ultra-thin and stretchable characteristics enable them to maintain high performance after encapsulation, while the ultra-thin characteristic means that encapsulation essentially has no impact on the sensor's performance. Waterproof structural adhesive was incorporated into the edge seams and wire areas of the encapsulated sensors, where water infiltration was a potential concern, to augment their waterproof capabilities.

The detailed implementation of the practical underwater intelligent communication system is shown in Fig. 5a. Deep learning techniques were used to classify the collected Morse code signals. The sensor differentiates between short pressure impulses (denoted by dots) and sustained pressure applications (denoted by dashes), which are combined to generate Morse code. For instance, three rapid taps encode an "S", while three long presses encode an "O", thereby enabling the transmission of the standard "SOS" distress signal (Fig. 5b). Beyond the transmission of basic signals, the conveyance of complex messages is facilitated by the rhythmic tapping of specific letter sequences (Figs. 5c and 5d). A dataset was constructed, incorporating both standard emergent codes (e.g., SOS) and specific command variants labelled HELP, HURRY (Figs. S6 and S7). A total number of 987 samples were accumulated. The raw sensor output was converted into image formats to serve as inputs for the neural network. A simplified convolutional neural network (CNN) was used for feature extraction and classification. The feature extraction part used a transfer learning method based on MobileNetV2. The training metrics showed excellent convergence on both the training and validation sets (Figs. 5e and 5f). The accuracy and loss were highly correlated. In addition, the confusion matrix derived from the test set confirmed superior performance, with zero misclassification (Fig. 5g). Despite the modest size of the current dataset, the outcomes of this study showed the feasibility of the proposed approach. We expect that further performance gains will be realized with the expansion of data collection.

In summary, the present study showed the broad potential of the sensor in the domains of underwater safety systems, health monitoring and intelligent communication interfaces. To verify the long-term

underwater stability of the sensor, a long-term output verification experiment of the sensor in a water tank was conducted. The experimental results (Fig. S8) showed that the sensor displays consistent output for

about 3 hours underwater, which fulfills the time requirements for single diving and associated activities. This aligns with the initial intended application

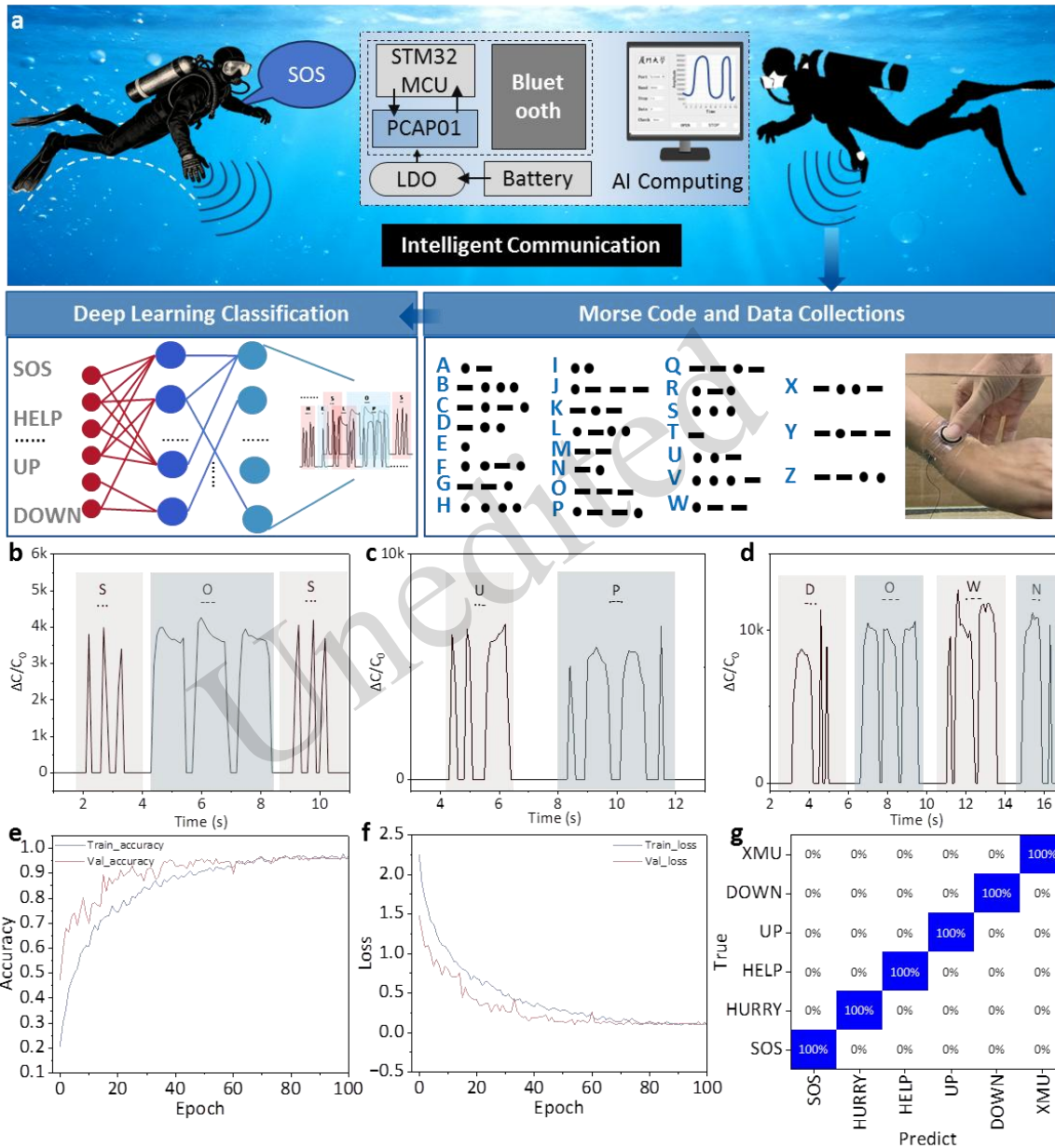


**Fig. 5 Underwater intelligent communication: (a) system design; (b-d) sensor output signal diagrams; (e-f) accuracy and loss curve during neural network training process; (g) test set confusion matrix**

scenario of the sensor, which pertains to short-term activities such as diving or swimming that may necessitate emergency communication.

#### 4 Conclusions

In summary, this study established a high-performance flexible pressure sensor by iontronic sensing principles and engineered micro-pyramidal architectures. The sensor was developed to achieve ultra-high sensitivity, rapid

response times, and exceptional operational stability by transitioning from traditional parallel-plate capacitive mechanisms to an EDLs model augmented by interfacial contact area modulation. Moreover, the integration of screen printing with molding provides a scalable fabrication strategy that is well-suited to mass production. The practical utility of the device was systematically validated across diverse domains. In precision healthcare, the sensor showed high-fidelity capture of human pulse waveforms, thereby facilitating the identification of optimal acquisition pressures for non-invasive monitoring. Following hermetic encapsulation, the technology was successfully adapted for aquatic environments. A novel underwater intelligent communication system was demonstrated, which combines tactile Morse code encoding with deep learning-assisted decoding, achieving high accuracy in signal classification. Collectively, this work underscores the immense potential of flexible iontronic sensors in bridging the gap between terrestrial healthcare and aquatic exploration, paving the way for next-generation HMI and cross-medium intelligent sensing systems.

### Acknowledgments

This work is funded by the National Natural Science Foundation of China (62274140, 62405294), Open Project Fund of Hubei Key Laboratory of Modern Manufacturing Quality Engineering (20250481), Open Research Fund Program of National Key Laboratory of Aerospace Chemical Power (NKLACP220241B14), the National Key Research and Development Program of China (2023YFB3208600), the Key Program of the National Natural Science Foundation of China (62433017), the Fundamental Research Funds for the Central Universities (20720230030), the Xiaomi Young Talents Program/Xiaomi Foundation, Shenzhen Science and Technology Program (JCYJ20230807091401003), Fundamental Research Program of Shanxi Province (202403021222157), Postgraduate research innovation Project of Shanxi Province (2024KY583), the International Science and Technology Joint Research Project of Hubei, China (2024EHA007).

### Author contributions

Menghui XIANG designed the research. Menghui XIANG and Cong ZHAI processed the corresponding data and wrote the first draft of the manuscript. Congcong Hao and Libo GAO revised and edited the final version. Guirong WU, Jin CHAI, Zekai HUANG, Mengran LIU, Lei NIE, Xiewen WEN, Yunlong ZHAO, Bin YAO, Heying ZHANG and Chenyang XUE helped to organize and revise the manuscript.

### Conflict of interest

The authors declare that they have no conflict of interest.

### References

- Yang ZK, Duan QK, Zang JB, et al., 2023. Boron nitride-enabled printing of a highly sensitive and flexible iontronic pressure sensing system for spatial mapping. *Microsystems & Nanoengineering*, 9(1):68. <https://doi.org/10.1038/s41378-023-00543-x>.
- Teng YY, Wang X, Zhang ZD, et al., 2024. Fully printed minimum port flexible interdigital electrode sensor arrays. *Nanoscale*, 16(15):7427–7436. <https://doi.org/10.1039/d3nr06664a>.
- Zhao YL, Yuan YB, Zhang HY, et al., 2024. A Fully Integrated Electronic Fabric-Enabled Multimodal Flexible Sensors for Real-Time Wireless Pressure-Humidity-Temperature Monitoring. *International Journal of Extreme Manufacturing*, 6(6):065502. <https://doi.org/10.1088/2631-7990/ad6aad>.
- Ren JY, Liu YH, Wang ZQ, et al., 2021. An Anti-Swellable Hydrogel Strain Sensor for Underwater Motion Detection. *Advanced Functional Materials*, 32(13):2107404. <https://doi.org/10.1002/adfm.202107404>.
- Zhu CJ, Chen GQ, Li SN, et al., 2024. Breathable Ultrathin Film Sensors Based on Nanomesh Reinforced Anti-Dehydrating Organohydrogels for Motion Monitoring. *Advanced Functional Materials*, 34(52):2411725. <https://doi.org/10.1002/adfm.202411725>.
- Zhang ZY, Yao AF and Raffa Patrizio, 2024. Transparent, Highly Stretchable, Self-Healing, Adhesive, Freezing-Tolerant, and Swelling-Resistant Multifunctional Hydrogels for Underwater Motion Detection and Information Transmission. *Advanced Functional Materials*, 34(49):2407529. <https://doi.org/10.1002/adfm.202407529>.
- Liang JW, Guo HJ, Sun LN, et al., 2025. A Nanocrack-Based Graphene/PDMS-Encapsulated Medical Tape Flexible Sensor for Motion Detection of Underwater Robots. *Advanced Materials Technologies*, 10(20):e00620. <https://doi.org/10.1002/admt.202500620>.
- Liu HD, Liu C, Luo JN, et al., 2024. Micromesh reinforced strain sensor with high stretchability and stability for full-range and periodic human motions monitoring. *InfoMat*, 6(4):e12511. <https://doi.org/10.1002/inf2.12511>.
- Lin SM, Li XR, Wu YJ, et al., 2025. Load-Bearing Piezoelectric Integrated Device with Inherent Stress Monitoring Capabilities. *Advanced Functional Materials*, 35(38): 2502346. <https://doi.org/10.1002/adfm.202502346>.
- Min Seongwook, Kim Dong Hyun, Joe Daniel J., et al., 2023. Clinical Validation of a Wearable Piezoelectric Blood-Pressure Sensor for Continuous Health

- Monitoring. *Advanced Materials*, 35(26):2301627. <https://doi.org/10.1002/adma.202301627>.
- Xiang QX, Zhao GJ, Tang T, et al., 2024. All-Carbon Piezoresistive Sensor: Enhanced Sensitivity and Wide Linear Range via Multiscale Design for Wearable Applications. *Advanced Functional Materials*, 35(15):2418706. <https://doi.org/10.1002/adfm.202418706>.
- Li ZW, Lv T, Wang XW, et al., 2025. High-Performance MXene/TPU Flexible Piezoresistive Sensors for Enhanced Gesture Recognition and Interactive Control Applications. *Advanced Materials Technologies*, 10(17):e00613. <https://doi.org/10.1002/admt.202500613>.
- Ma R, Zhao YL, Chen HB, et al., 2023. Highly Sensitive Flexible Capacitive Pressure Sensor with Porous Hierarchical Structure Realized by a Microwave Curing Method. *Advanced Engineering Materials*, 26(2):2301412. <https://doi.org/10.1002/adem.202301412>.
- Liu LT, Mo LX, Han SB, et al., 2025. Enhancing Flexible Capacitive Sensor Performance through the Synergy of Thermally Expandable Microspheres and Carbon Nanotubes via 3D Direct Ink Writing. *Advanced Functional Materials*, e14093. <https://doi.org/10.1002/adfm.202514093>.
- Chang H, Zhao JZ, Qin R, et al., 2025. Ultra-Wideband Hybrid Triboelectric–Piezoelectric Acoustic Sensors Enabled by Acoustic Metasurface Lens for Environment Perception and Medical Imaging. *Advanced Functional Materials*, e13202. <https://doi.org/10.1002/adfm.202513202>.
- Sun HL, Li XY, Zhao ZH, et al., 2025. Kirigami Cube-Inspired Triboelectric Vector Sensor for Human–Machine Interaction. *Advanced Functional Materials*, e16876. <https://doi.org/10.1002/adfm.202516876>.
- Li KX, Xu TL, Zhou JY, et al., 2025. Flexible capacitive pressure sensor with chemically reduced graphene oxide on a pyramid-structured melamine sponge array by laser engraving. *Journal of Materials Chemistry C*, 13(41):21215–21226. <https://doi.org/10.1039/d5tc00563a>.
- Kurup Lekshmi A., Arthur Joshua N. and Yambem Soniya D., 2022. Highly Sensitive Capacitive Low-Pressure Graphene Porous Foam Sensors. *ACS Applied Electronic Materials*, 4(8):3962–3972. <https://doi.org/10.1021/acsaelm.2c00616>.
- Nie BQ, Li RY, Cao J, et al., 2015. Flexible Transparent Iontronic Film for Interfacial Capacitive Pressure Sensing. *Advanced Materials*, 27(39):6055–6062. <https://doi.org/10.1002/adma.201502556>.
- Nie BQ, Xing SY, Brandt James D, et al., 2012. Droplet-based interfacial capacitive sensing. *Lab on a Chip*, 12(6):1110–1118. <https://doi.org/10.1039/c2lc21168h>.
- Guo JH, Niu Q, Xu JL, et al., 2025. All-In-One Iontronic Sensing Aligner for High-Precision 3D Orthodontic Force Monitoring. *Advanced Science*, 12(43):e11984. <https://doi.org/10.1002/advs.202511984>.
- Cheng Y, Guo CH, Li S, et al., 2022. Aquatic Skin Enabled by Multi-Modality Iontronic Sensing. *Advanced Functional Materials*, 32(48):2205947. <https://doi.org/10.1002/adfm.202205947>.
- Yang ZK, Zhao YL, Lan YH, et al., 2024. Screen-Printable Iontronic Pressure Sensor with Thermal Expansion Microspheres for Pulse Monitoring. *ACS Applied Materials & Interfaces*, 16(30):39561–39571. <https://doi.org/10.1021/acsami.4c05688>.
- Yang QQ, Ye ZQ, Wu RK, et al., 2023. A Highly Sensitive Iontronic Bimodal Sensor with Pressure–Temperature Discriminability for Robot Skin. *Advanced Materials Technologies*, 8(21):2300561. <https://doi.org/10.1002/admt.202300561>.
- Yang QQ, Li BQ, Wang MK, et al., 2025. Machine Learning-Enhanced Modular Ionic Skin for Broad-Spectrum Multimodal Discriminability in Bidirectional Human–Robot Interaction. *Advanced Materials*, 37(42):e08795. <https://doi.org/10.1002/adma.202508795>.
- Zhao YL, Sun QX, Mei SX, et al., 2024. Wearable multichannel-active pressurized pulse sensing platform. *Microsystems & Nanoengineering*, 10(1):77–86. <https://doi.org/10.1038/s41378-024-00703-7>.
- Yang CX, Hu JF, Liu LH, et al., 2024. An underwater vest containing an antioxidant MXene hydrogel for sensitive recognition of fish locomotion. *Microsystems & Nanoengineering*, 10(1):41–57. <https://doi.org/10.1038/s41378-024-00675-8>.
- Zhao JW, Hu Q, Fu TQ, et al., 2024. Capacitive Low-Frequency Hydrophone Based on Micronanostructured Iontronic Hydrogel for Underwater Monitoring. *ACS Nano*, 18(33): 22010–22020. <https://doi.org/10.1021/acsnano.4c04094>.
- Xiang MH, Yu LF, Chai J, et al., 2025. An iontronic pressure sensor with high linearity and ultrawide range over 4 MPa for submarine pressure monitoring. *Chemical Engineering Journal*, 517:164365. <https://doi.org/10.1016/j.cej.2025.164365>.
- Wang YH, Xiang MH, Li JH, et al., 2024. Highly Sensitive Flexible Iontronic Pressure Sensor for Marine Pressure Monitoring. *IEEE Electron Device Letters*, 45(12):2530–2533. <https://doi.org/10.1109/led.2024.3474909>.
- Guo XH, Zhao JG, Hu B, et al., 2024. Flexible Pressure Sensor With High Sensitivity and Fast Response Based on Bionic Honeycomb-Structured Polydimethylsiloxane/Aluminum Oxide Composites Dielectric via 3-D Printing. *IEEE Transactions on Electron Devices*, 71(7):4283–4291. <https://doi.org/10.1109/ted.2024.3401653>.
- Lu P, Wang L, Zhu P, et al., 2021. Iontronic pressure sensor with high sensitivity and linear response over a wide pressure range based on soft micropillared electrodes.

*Science Bulletin*, 66(11):1091–1100.

<https://doi.org/10.1016/j.scib.2021.02.019>.

Jin QX, Wang CY, Wu H, et al., 2024. 3D Printing of Capacitive Pressure Sensors with Tuned Wide Detection Range and High Sensitivity Inspired by Bio-Inspired Kapok Structures. *Macromolecular Rapid Communications*, 45(9):2300668.

<https://doi.org/10.1002/marc.202300668>.

Hong WQ, Guo XH, Zhang TX, et al., 2023. Flexible Capacitive Pressure Sensor with High Sensitivity and Wide Range Based on a Cheetah Leg Structure via 3D Printing. *ACS Applied Materials & Interfaces*, 15(39):46347–46356.

<https://doi.org/10.1021/acsami.3c09841>.

Lv CY, Tian CC, Jiang JS, et al., 2023. Ultrasensitive Linear Capacitive Pressure Sensor with Wrinkled Microstructures for Tactile Perception. *Advanced Science*, 10(14):2206807.

<https://doi.org/10.1002/advs.202206807>.

Wang X, Wu GR, Zhang XK, et al., 2024. Traditional Chinese Medicine (TCM)-Inspired Fully Printed Soft Pressure Sensor Array with Self-Adaptive Pressurization for Highly Reliable Individualized Long-Term Pulse Diagnostics. *Advanced Materials*, 37(1):2410312.

<https://doi.org/10.1002/adma.202410312>.

Yang J, Liu Q, Deng Z., et al., 2019. Ionic liquid-activated wearable electronics. *Materials Today Physics*, 8:78–85.

<https://doi.org/10.1016/j.mtphys.2019.02.002>.

Cetin Oyku, Cicek Melih Ogeday, Cugunlular Murathan, et al., 2024. MXene-Deposited Melamine Foam-Based Iontronic Pressure Sensors for Wearable Electronics and Smart Numpads. *Small*, 20(45):2403202.

<https://doi.org/10.1002/sml.202403202>.

## Electronic supplementary materials

Figs. S1–S8

## 中文概要

**题目:** 用于脉搏信号检测和水下智能通信的高灵敏度柔性离电式压力传感器

**作者:** 向梦辉<sup>1,2</sup>, 翟聪<sup>2</sup>, 郝聪聪<sup>3</sup>, 吴贵荣<sup>1</sup>, 柴进<sup>2,4</sup>, 赵云龙<sup>1</sup>, 黄泽凯<sup>1</sup>, 姚斌<sup>1,2</sup>, 张鹤赢<sup>3</sup>, 刘梦然<sup>5</sup>, 聂磊<sup>5</sup>, 温燮文<sup>6</sup>, 薛晨阳<sup>1,2</sup>, 高立波<sup>1</sup>

**机构:** <sup>1</sup>厦门大学, 萨本栋微米纳米科学技术研究院&智能仪器与装备, 中国厦门, 361102; <sup>2</sup>崂山实验室, 中国青岛, 266237; <sup>3</sup>中北大学仪器科学与动态测试教育部重点实验室, 中国太原, 030051; <sup>4</sup>厦门大学, 化学与化学工程学

院, 中国厦门, 361102; <sup>5</sup>湖北工业大学, 机械工程学院&湖北省现代制造数量工程重点实验室, 中国武汉, 430068; <sup>6</sup>香港理工大学, 工业与系统工程系&3D打印研究所&超精密加工技术国家重点实验室, 中国香港, 999077

**目的:** 柔性压力传感器已成为可穿戴电子设备、水下监测和人机界面发展的关键。然而, 开发能够在陆地和水下环境中无缝运行的统一传感平台仍然是一个挑战。

**创新点:** 1. 传感器结合金字塔微结构和离电式感知机理获得了高灵敏度 (370 kPa<sup>-1</sup>)、快速响应/恢复时间 (20 ms) 等优异性能; 2. 传感器可实现可穿戴健康监测领域及水下智能通讯领域的双重应用。

**方法:** 传感器敏感层基于倒模方法制造, 敏感材料由碳纳米管、离子液体及聚氨酯等材料混合而成, 辅以丝网印刷等工艺进行传感器的制备。

**结论:** 在可穿戴健康监测领域, 该传感器展示了辨别微弱人体脉搏信号的能力。结合中国传统脉诊方法, 可以确定最佳取脉压力点, 进而促进高保真脉搏波形的采集。同时, 在水下智能通信领域, 传感器可用于采集莫尔斯电码信号, 并可通过深度学习算法对其进行准确分类。这项工作不仅验证了传感器的高性能, 还展示了其双重功能, 将人类医疗保健与智能水下交互无缝连接, 显著扩大了柔性传感技术的应用范围。

**关键词:** 柔性压力传感器; 水下传感; 离电式传感器; 机器学习